Numerical Modeling of Mineral Dissolution in Acidic Environments: A Step Towards Advancing CCS Applications

Kristian Nascimento Telöken[1,2] Marcos Antonio Klunk[2]

Adolpho Herbert Augustin[2] Henrique Serrat[2]

Tiago Jonatan Girelli[2] Farid Chemale Jr[2]

[1] Programa de Pós Graduação em Engenharia Mecânica, Universidade Federal do Rio Grande do Sul (UFRGS)
[2] Universidade do Vale do Rio dos Sinos (UNISINOS)

1 Supplementary Material

1.1 Geometry

The geometry used for the first two parts of the study is shown in Fig. 1. It includes the dimensions of the domain as well as the boundary conditions for the flow.

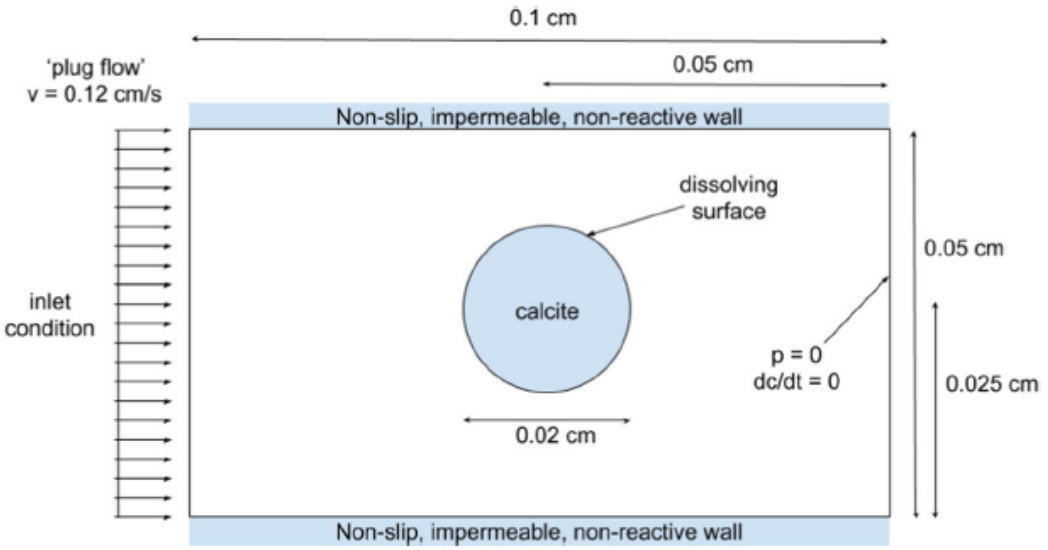

Figure 1: Computational domain and boundary conditions for parts I and II. Source: Molins et al. (2021).

The geometry for the third case, involving the experimental study, was generated from a mask image, Fig. 2.

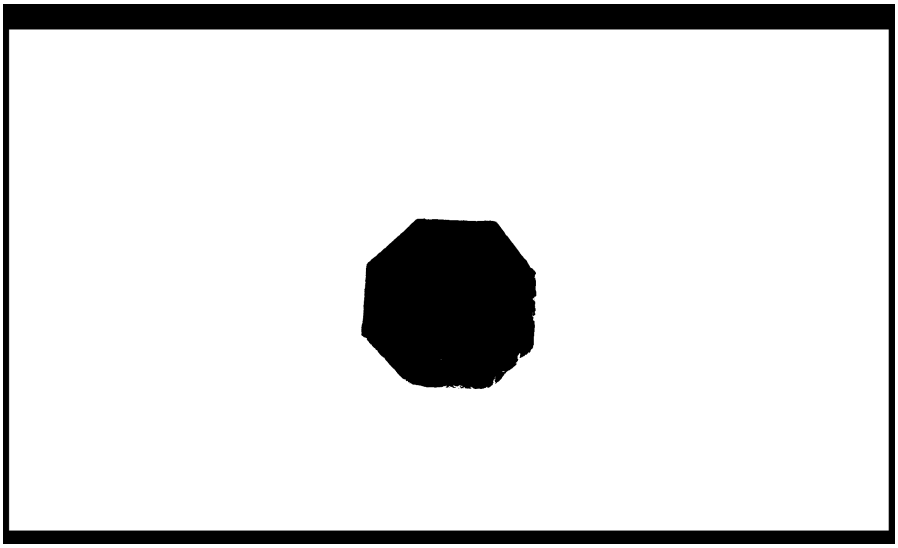

Figure 2: Masking image (grain in black). Source: Molins et al. (2021).

The geometry has dimensions of 2.6 mm × 1.5 mm × 0.2 mm, accurately representing the domain of the figure with a 3D expansion of 0.2 mm.

1.2 Mathematical Model

The simulation of multicomponent reactive flow involves solving the transport equations for each chemical species, including reaction source terms and diffusive fluxes. This section describes the fundamental mathematical expressions used to represent the conservation of mass for chemical species, reaction rates, and kinetic expressions.

1.2.1 Species Conservation Equation

The conservation of mass for a diffusing species i is described by:

$$\frac{\partial}{\partial t}(\rho Y_i) + \nabla \cdot (\rho \vec{v} Y_i) = -\nabla \cdot \vec{J_i} + R_i + S_i$$

where:

- ρ is the mixture density,
- $\vec{v}$ is the velocity vector of the diffusing species,
- Y_i is the mass fraction of species i,
- $\vec{J_i}$ is the diffusive flux of species i,
- R_i is the net rate of production of species i by chemical reaction,
- S_i is the rate of creation by dispersed phases or user-defined sources.

1.2.2 Reaction Source Term

The net production rate R_i of species i due to chemical reactions is calculated as:

$$R_i = M_{w,i} \sum_{r=1}^{N_R} \varepsilon \, \hat{R}_{i,r}$$

where:

- $M_{w,i}$ is the molecular weight of species i,
- ε is the porosity,

- $\hat{R}_{i,r}$ is the molar rate of creation or destruction of species i in reaction r,
- N_R is the number of chemical reactions.

1.2.3 General Reaction Form

Each chemical reaction is represented in stoichiometric form as:

$$\sum_{i=1}^{N} \nu'_{i,r} \mathcal{M}_i \underset{k_{b,r}}{\overset{k_{f,r}}{\rightleftharpoons}} \sum_{i=1}^{N} \nu''_{i,r} \mathcal{M}_i$$

where:

- N is the number of chemical species,
- $\nu'_{i,r}$ and $\nu''_{i,r}$ are the stoichiometric coefficients of reactants and products in reaction r,
- $\mathcal{M}_i$ denotes the chemical species i,
- $k_{f,r}$ and $k_{b,r}$ are the forward and backward rate constants of reaction r.

1.2.4 Molar Rate of Reaction

The molar rate of production or consumption of species i in reaction r is given by:

$$\hat{R}_{i,r} = \Gamma \left(\nu''_{i,r} - \nu'_{i,r} \right) \left[k_{f,r} \prod_{j=1}^{N} [C_{j,r}]^{\eta'_{j,r}} - k_{b,r} \prod_{j=1}^{N} [C_{j,r}]^{\eta''_{j,r}} \right]$$

where:

- $C_{j,r}$ is the molar concentration of species j in reaction r,
- $\eta'_{j,r}$ and $\eta''_{j,r}$ are the rate exponents for reactant and product species,
- Γ is a geometric or scaling factor (e.g., porosity or phase fraction).

1.2.5 Arrhenius Expression for Reaction Rates

The forward rate constant for reaction r, $k_{f,r}$, is determined using the Arrhenius expression:

$$k_{f,r} = A_r T^{\beta_r} \exp\left(-\frac{E_r}{RT} \right)$$

where:

- A_r is the pre-exponential factor (units depend on reaction order),
- β_r is the temperature exponent (dimensionless),
- E_r is the activation energy (J/mol),
- R is the universal gas constant (J/mol·K),
- T is the absolute temperature (K).

1.3 User Defined Function UDF

1.3.1 Dissolution Rate

The dissolution rate (R_{diss}) of calcite is modeled as a first-order kinetic reaction proportional to the H^+ concentration and is given by:

$$R_{\text{diss}} = k \cdot C_{H^+} \cdot \gamma$$

where:

- k: Reaction rate constant ($8.91 \times 10^{-4}\,\text{kmol/m}^2 \cdot \text{s}$).
- C_{H^+}: H^+ concentration (kmol/m^3).
- γ: Activity coefficient ($1\,\text{m}^3/\text{kmol}$).

This rate represents the molar flux of calcite dissolved per unit area per unit time.

1.3.2 Physical Displacement Rate

The molar dissolution rate is converted to a physical displacement rate (v_{diss}) of the calcite surface (in m/s) by accounting for the molar mass and density of calcite:

$$v_{\text{diss}} = \frac{R_{\text{diss}} \cdot M_{CaCO_3}}{\rho_{CaCO_3}}$$

where:

- R_{diss}: Dissolution rate ($\text{kmol/m}^2 \cdot \text{s}$).
- M_{CaCO_3}: Molar mass of calcite ($100\,\text{kg/kmol}$).
- ρ_{CaCO_3}: Density of calcite ($2710\,\text{kg/m}^3$).

This displacement rate represents the velocity at which the calcite surface shrink due to dissolution.

1.3.3 Node Displacement

The displacement of the mesh nodes (Δ) per timestep is calculated by multiplying the displacement rate by the timestep size (Δt) and applying a safety factor of 0.5 to reduce numerical instability:

$$\Delta = v_{\text{diss}} \cdot \Delta t \cdot 0.5$$

To prevent excessive mesh deformation, the displacement is capped at the maximum allowable value ($\Delta_{\max} = 1 \times 10^{-5}\,\text{m}$):

$$\Delta = \begin{cases} \Delta_{\max} & \text{if } \Delta > \Delta_{\max}, \\ -\Delta_{\max} & \text{if } \Delta < -\Delta_{\max}, \\ \Delta & \text{otherwise.} \end{cases}$$

1.3.4 Surface Normal and Node Movement

For each face on the calcite surface, the UDF computes the face normal vector ($\vec{n}$) and its magnitude (area, A) using the Fluent macro `F_AREA(normal, f, t)`. The unit normal vector ($\hat{n}$) is calculated as:

$$\hat{n} = \frac{\vec{n}}{A}$$

The nodes of the face are displaced in the direction of the unit normal vector. For a node at position (x, y, z), the new coordinates after displacement are:

$$x_{\text{new}} = x + \Delta \cdot \hat{n}_x$$

$$y_{\text{new}} = y + \Delta \cdot \hat{n}_y$$

$$y_{\text{new}} = z + \Delta \cdot \hat{n}_z$$

where $\hat{n}_x$, $\hat{n}_y$ and $\hat{n}_z$ are the x-, y- and z-components of the unit normal vector, and the displacement is applied in 2D for the first two parts and in 3D for the last.

1.4 Results

In the first part, the simulation of reactive flow without geometric evolution was conducted on a two-dimensional domain. The results showed in Fig. 3, that the Fluent model accurately captured average dissolution rate when compared with the data from Molins et al. (2021), revealing the good agreement with the others codes. In Fig. 4, it is possible to observe a significant difference between the behavior of Fluent and the other models. This is due to the domain initialization approach: in order to keep the dissolution rate at zero at the beginning of the simulation and to capture its increase over time, the domain was initialized without the presence of the H^+ ion, which becomes present only through its concentration in the influent at the inlet.

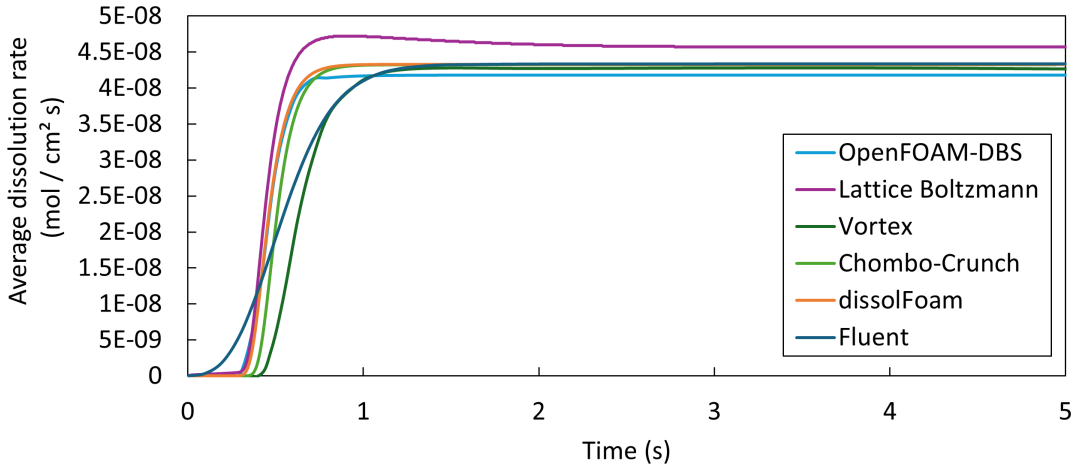

Figure 3: Evolution of the average reaction rate, for OpenFOAM-DBS, Lattice-Boltzmann, Vortex, Chombo-Crunch, dissolFoam and Fluent simulations. Adapted from: Molins et al. (2021).

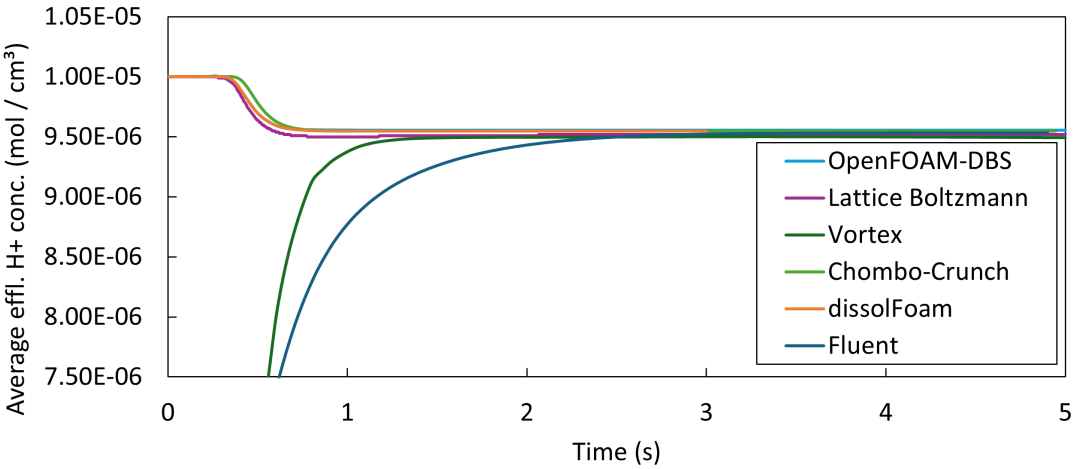

Figure 4: Evolution of the effluent concentration, for OpenFOAM-DBS, Lattice-Boltzmann, Vortex, Chombo-Crunch, dissolFoam and Fluent simulations. Adapted from: Molins et al. (2021).

The contours for this first part are shown in Fig. 5, together with the results from Molins et al. (2021). Fig. 6 presents the results obtained in this study, again showing good agreement with the cases presented by the author.

In the second part, the geometric evolution of calcite was incorporated, enabling the analysis of physical dissolution in two dimensions. The implemented UDFs adjusted the sample geometry based on the dissolution rate and H^+ concentration. Resulting in surface area reduction of the calcite, with good agreement with others softwares, Fig. 7 , and visible changes in the shape over time, Fig. 8.

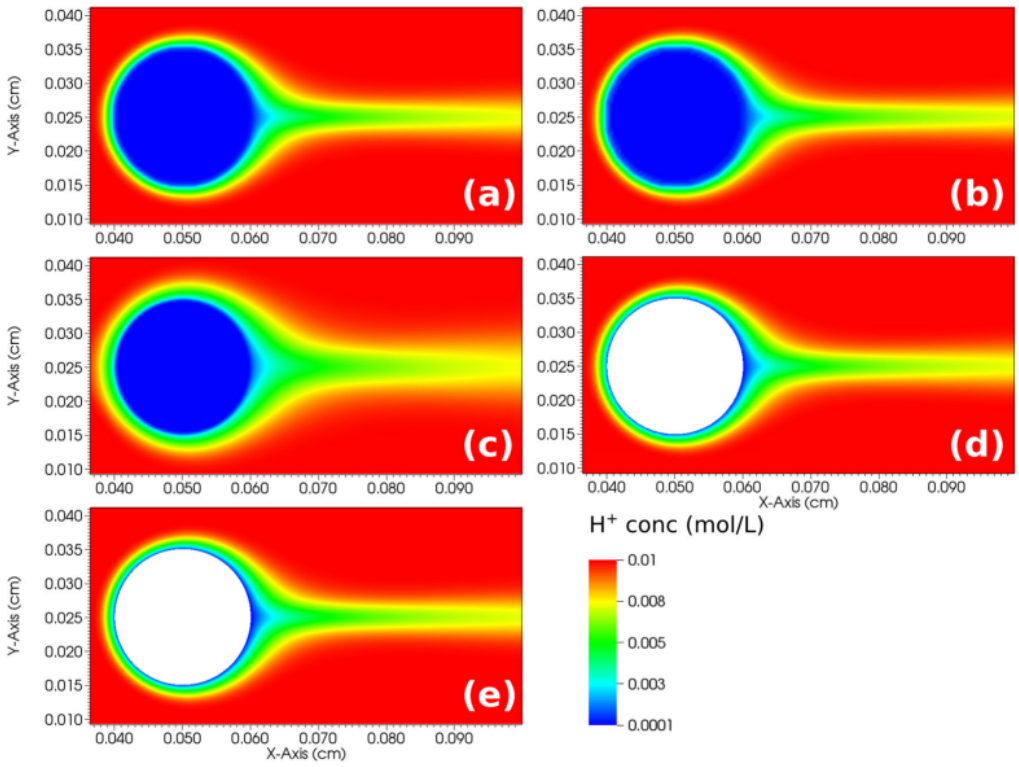

Figure 5: Concentration contours for the two-dimensional dissolution of a cylindrical calcite grain obtained from: a) OpenFOAMDBS, b) lattice Boltzmann, c) vortex, d) Chombo-Crunch, and e) dissol-Foam. Source: Molins et al. (2021).

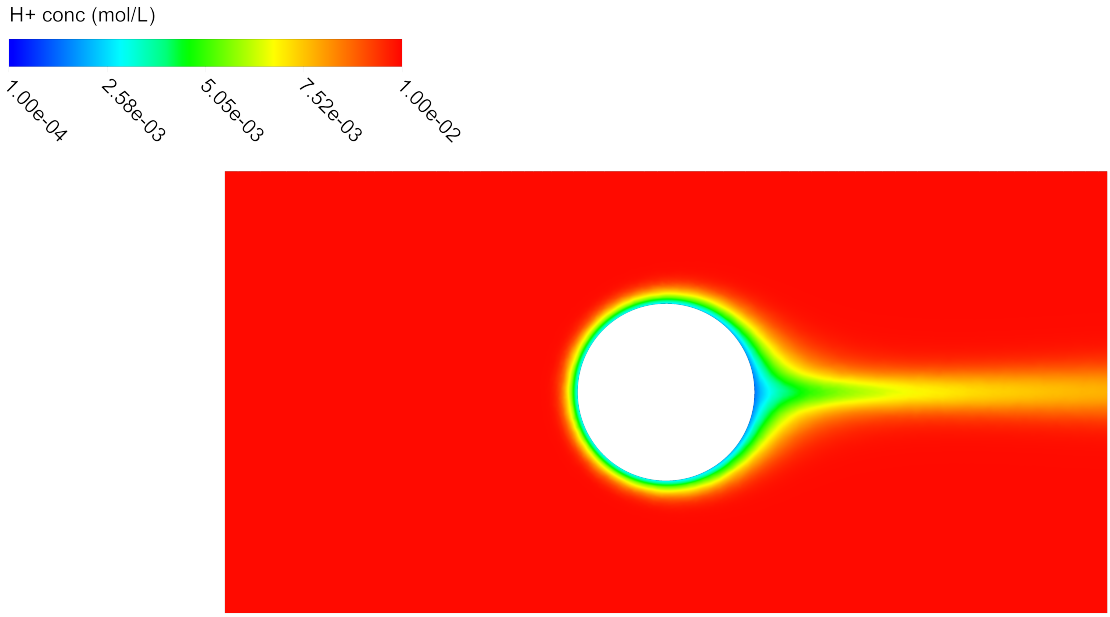

Figure 6: Concentration contour for the two-dimensional dissolution of a cylindrical calcite grain obtained from Fluent.

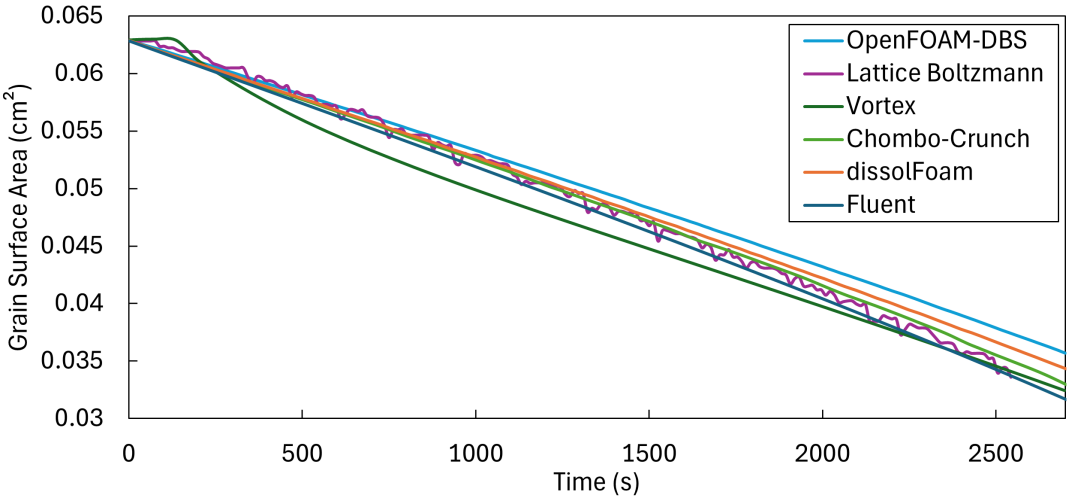

Figure 7: Evolution of the surface area as a function of time during the dissolution of a two-dimensional disk in part II, for OpenFOAM-DBS, Lattice-Boltzmann, Vortex, Chombo-Crunch, dissolFoam and Fluent simulations Adapted from: Molins et al. (2021).

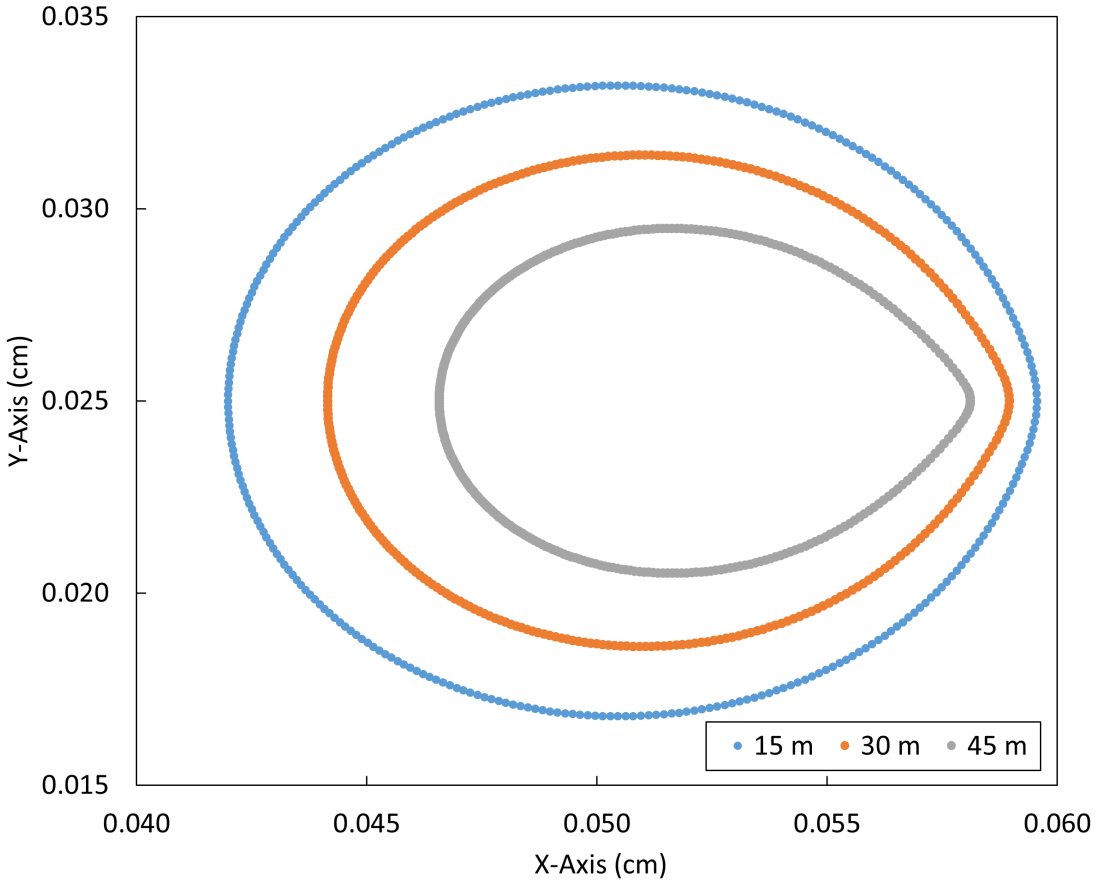

Figure 8: Evolution of the shape of the calcite grain over time in 15, 30 and 45 minutes.

In the third part, the model was extended to a three-dimensional geometry, and the results were directly compared with experimental data and reference simulations. In this stage, ANSYS Fluent stood out by achieving great agreement with the experiments, whereas some of the other codes exhibited deviations of the experimental results, Fig. 9.

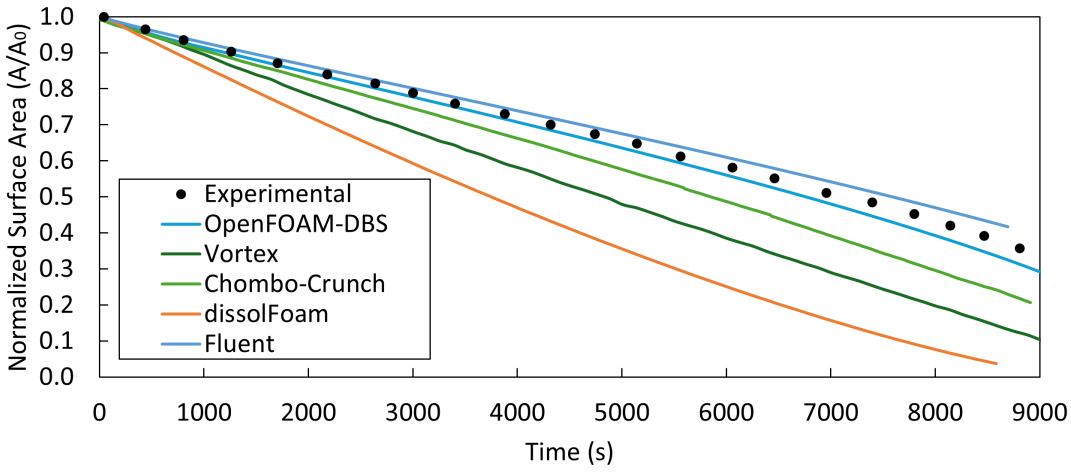

Figure 9: Evolution of the surface area obtained from part III. Experimental results (dots) can be compared with simulations for OpenFOAM-DBS, Vortex, Chombo-Crunch, dissolFoam and Fluent. Adapted from: Molins et al. (2021).

References

[1] Molins, S., Soulaine, C., Prasianakis, N. I., et al. (2021). Simulation of mineral dissolution at the pore scale with evolving fluid-solid interfaces: review of approaches and benchmark problem set. *Computational Geosciences*, 25, 1285–1318. https://doi.org/10.1007/s10596-019-09903-x